JOURNAL OF CHEMICAL INFORMATION AND MODELING

Article

pubs.acs.org/jcim

A Pragmatic Approach Using First-Principle Methods to Address Site of Metabolism with Implications for Reactive Metabolite Formation

Ya-Wen Hsiao,[†] Carl Petersson,[†] Mats A. Svensson,[†] and Ulf Norinder*[,†,‡]

[†]AstraZeneca Research and Development Södertälje, SE-151 85 Södertälje, Sweden

[‡]Department of Pharmacy, Uppsala University, SE-751 23 Uppsala, Sweden

Supporting Information

ABSTRACT: A majority of xenobiotics are metabolized by cytochrome P450 (CYP) enzymes. The discovery of drug candidates with low propensity to form reactive metabolites and low clearance can be facilitated by understanding CYP-mediated xenobiotic metabolism. Being able to predict the sites where reactive metabolites form is beneficial in drug design to produce drug candidates free of reactive metabolite issues. Herein, we report a pragmatic protocol using first-principle density functional theory (DFT) calculations for predicting sites of epoxidation and hydroxylation of aromatic substrates mediated by CYP. The method is based on the relative stabilities of the CYP-substrate intermediates or the substrate epoxides. Consequently, it concerns mainly the electronic reactivity of the substrates. Comparing to the experimental findings, the presented protocol gave excellent first-ranked epoxidation site predictions of 83%, and when the test was extended to CYP-mediated sites of aromatic hydroxylation, satisfactory results were also obtained (73%). This indicates that our assumptions are valid and also implies that the intrinsic reactivities of the substrates are in general more important than their binding poses in proteins, although the protocol may benefit from the addition of docking information.

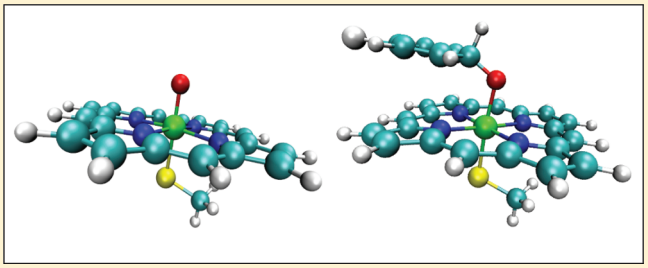

INTRODUCTION

In view of the compelling evidence linking formation of reactive metabolites to toxicity for numerous drugs, formation of such metabolites is considered a liability in candidate drugs.[1] Screening methods for the formation of reactive intermediates via cytochrome P450 (CYP)-mediated metabolism have been developed and deployed within the pharmaceutical industry[2] to avoid formation of reactive metabolites. A challenge in medicinal chemistry is to design drug candidates without this liability. The strategies used depend on the mechanism which the metabolites form and the site of metabolism (SOM). Most methods for reactive metabolite screening are based on or can be combined with mass spectrometry; they provide information on the molecular weight of formed adducts of reactive species. Combining information on the structure of the parent drug and data on the molecular weight of the formed adduct generally allows classification of the mechanism of reactive intermediate formation. However, in order to fully exploit this knowledge in design of molecules devoid of reactive metabolite liabilities, information on the SOM is also required. As current methods are based on mass spectrometry, the exact SOM or even the region of the molecule being involved in the formation of the reactive species may be difficult to assign. To generate finite data on the SOM, more elaborate experiment utilizing NMR is often necessary. Such experiments are difficult to perform within a typical design−make−test cycle, as they require relatively large quantities of reactive metabolites to be produced.

One of the most common mechanisms of reactive metabolite formation is epoxide formation. The aim of this article is not to predict whether a xenobiotic will form a reactive metabolite or not but rather to identify where the resulting reactive metabolites are formed in order to guide drug design. Typical strategies to avoid the formation of reactive species via this mechanism include changing the electronics of the oxidized ring system, introduction of a metabolic soft-spot and/or a steric block of the SOM adjacent to the bond forming an epoxide.[3] All these strategies require knowledge on the SOM. In this work, we present an efficient first-principle in silico protocol to predict sites of CYP-mediated arene oxidation of drugs. To this end, we used mainly density functional theory (DFT) calculations without involving any rule derivation or trend fitting.

For the CYP-mediated reactions, the putative active species involved in the arene oxidation is generally accepted to be an oxoiron(IV) porphyrin radical cation, called compound I, shown in Figure 1. The rate-limiting step for aromatic oxidation has been suggested, both experimentally and theoretically, to be the creation of the bond between the iron-bound oxygen in compound I and SOM of the substrate, i.e., the formation of the tetrahedral σ-intermediate[4−6] (Figure 1). Quantum mechanical (QM) methods have been employed in earlier studies to locate the corresponding transition state of such complex and evaluate the activation energies for determining the SOM, either directly,

Received: November 1, 2011
Published: February 2, 2012

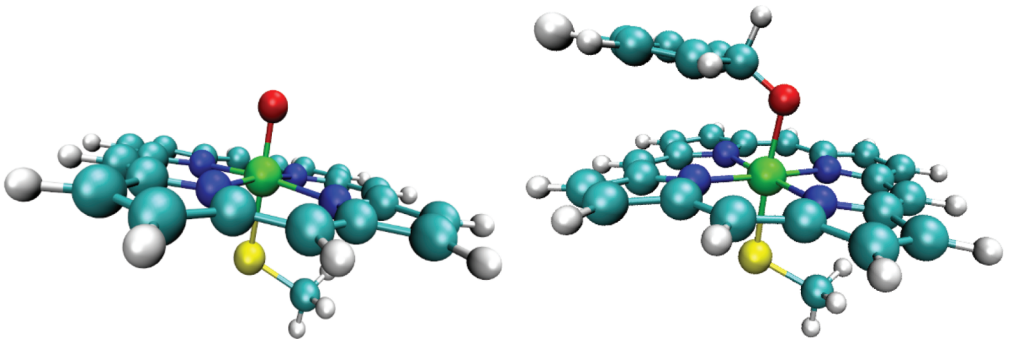

Figure 1. Structures of compound I (left) and σ-intermediate with face-on addition of the substrate (right). For clarity, side chains on the porphyrin are cut, and the iron-bound cysteine is simplified with $-SCH_3$. Fe is shown in green, N in blue, C in cyan, O in red, S in yellow, and H in white.

using semiempirical methods, or via generalized rule-making approaches if higher level methods were used.[7] However, the calculations of transition states are far from being trivial and quite difficult for complicated systems. In addition, the reliability and applicability of rule-based methods depend heavily on the completeness of the training set molecules; whether all possible chemical diversities are included, also the number of rules can easily grow and become too complicated to be useful.

Instead of searching for the transition states of σ-intermediates of a given substrate, we used the relative stabilities of the intermediates to determine the most viable site of its formation, which would be followed by subsequent epoxidation or hydroxylation. Since there is very little structural reorganization from the transition state to the intermediate, using the intermediate to depict the transition state fulfills the condition for applying the Hammond–Leffler postulate.[8,9] Further extrapolating the postulate, we also tested the possibility of using the relative stabilities of epoxides or hydroxides to replace the transition-state energies. DFT calculations were applied on model systems where compound I has been greatly simplified, so that the protocol was still affordable for many studies within a reasonable time frame.

The present approach focuses on characterizing the intrinsic electronic reactivity of the ligand, rather than the ligand poses in the enzymes. It has been pointed out by earlier work[10] that the intrinsic electronic reactivity is more important when performing tests using both ligand- and docking-based approaches. Hence we expect that through the study of the stabilization energies of the relevant molecules, a good prediction of the SOM may be achieved.

The performance of these two approaches were determined by comparing predictions with the experimental observations of 29 molecules for epoxidation and 30 molecules for arene hydroxylation.

METHOD AND COMPUTATIONAL DETAILS

Our site prediction protocol consists of the following steps and assumptions:

(1) Only the most solvent-exposed carbon atoms within the molecule are investigated with QM methods.
(2) Assume that the activation energies correlate with the stabilization energies of the σ-intermediates, following the Hammond–Leffler postulate, since very little structural reorganization is expected during the conversion from the transition state to the intermediate.
(3) Extend assumption 2 so that the energies of the arene oxidation products, i.e., epoxide or hydroxide, may also correlate to the activation energies.
(4) Simplify the σ-intermediate with model adducts for fast computations.

The stabilization energy (E_{stab}) for a carbon site i is given by

$$E_{\mathrm{stab}_i} = E_{\sigma_i} - E_{\mathrm{substrate}} - E_{\mathrm{probe}} \quad (1)$$

where E_{σ_i} and E_{probe} are the calculated energies of the model σ-intermediate formed at carbon site i and the probe (H/OCH_3/O, see below), respectively. Since the comparisons are performed for selected carbon sites of the same molecule for each probe, the last two terms in eq 1 remain constant. Therefore, in practice, only the energy of the σ-intermediate at each carbon site, E_{σ_i}, is used to make comparisons. The work flow is also shown in Scheme 1 using coumarin as an example. In this way,

Scheme 1. SOM Prediction Protocol Using QM Calculations

(1.) Pick 2 carbon atoms per ring with largest SASA: e.g., coumarin: C1, C2 and C9, C10.

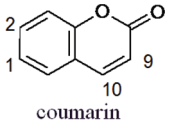

coumarin

(2.) Form adducts (H/OMe/O) at C1, C2, C9, C10. Optimize geometries using QM.

(3.) For each probe (H/OMe/O), find the most stable adduct which corresponds to the SOM/epoxide.

(4.) Apply 1-3 to new molecules to determine the prediction performance of each probe.

our method has the first-principle accuracy in describing the intrinsic reactivity for any substrate of interest via searching for energy minima. The complicated transition-state search is avoided, hence the needed computation time and resources are reduced.

The solvent accessible surface area (SASA) was used for the atom preselection. Areaimol[11] from the CCP4 program suite[12] was used to evaluate the SASA value of each atom. To exaggerate the SASA difference among atoms, hence make the choice of the most solvent exposed sites apparent, a probe radius of 25 Å, the upper limit in the program, was used. Two carbon atoms with the largest SASA per aromatic ring were chosen for the subsequent QM calculations of the σ-intermediates. The choice of two atoms per ring was rather arbitrary. However, we found it satisfactory as it was able to include all the major SOM of the

dx.doi.org/10.1021/ci200523f | J. Chem. Inf. Model. 2012, 52, 686–695

molecules in our test sets. There were cases where all atoms gave zero SASA values due to the large and thus insensitive probe, then a smaller probe radius of 1.4 Å was used to identify the candidate sites.

For the QM calculations, we first modeled these σ-intermediate by substituting the iron-oxo porphyrin with a methoxy radical. This surrogate model has been used in several earlier studies;[5,13−15] the DFT activation energies calculated with the methoxy radical have been found to correlate well (r^2 = 0.79) with those obtained with the full compound I model.[15] In addition, we further tested a yet more simplified model by using a hydrogen atom, also a radical, to replace the methoxy radical. We then compared the predictions to the experiments using these two models.

All QM calculations were performed with DFT using the Gaussian 09 package[16] with its default B3LYP functional[17,18] implementation, in combination with the 6-31G(d,p)[19−21] basis set. Structure of each substance was first optimized in vacuum, followed by a single point energy calculation to include the aqueous solvation effects with the polarizable continuum model,[22] at the optimized geometry. The relative gas phase energies for most of the systems were in the same ranking order as the relative solvated energies except for a few examples. In those cases, comparisons were made for geometries optimized with solvation effects included.

The addition of the substrate to compound I may follow two different pathways, namely face- or side-on additions, as shown in Figure 2. No consensus has been reached to which mode is

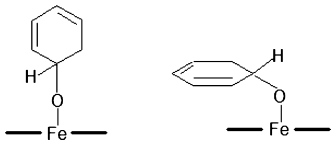

Figure 2. Substrate side- (left) or face-on addition (right) onto CYP.

favored by the enzyme. Therefore, we took both possibilities into account when using the methoxy radical adduct to model the σ-intermediate. We calculated both possible conformations of the complexes for each atom as well as both possible hydrogen orientations of the substrate for addition (e.g., A and B shown in Figure 3), then chose the σ-complex with the lowest energy to represent the site. On the other hand, using hydrogen radical as the model forms only one conformer, since it is just a point in space, thus circumventing the multiple computations and leads to a more efficient protocol.

The stability of σ-intermediate was evaluated atom-wise for two atoms per ring, but for epoxide calculations, both neighboring atoms to each chosen site were considered. All DFT calculations were accomplished within a reasonable time span ranging from minutes to hours.

RESULTS AND DISCUSSION

It might appear straightforward to choose the site which is the most stable energetically. However, while the level of QM method we used is satisfactory for most of the common applications, it is well recognized that the method is inadequate to discern small energy differences. Therefore, we considered sites with an energy difference less than 0.5 kcal/mol equally possible of being the SOM.

A set of 29 molecules shown in Figure 4 with available experimental data was used to test the present protocol for

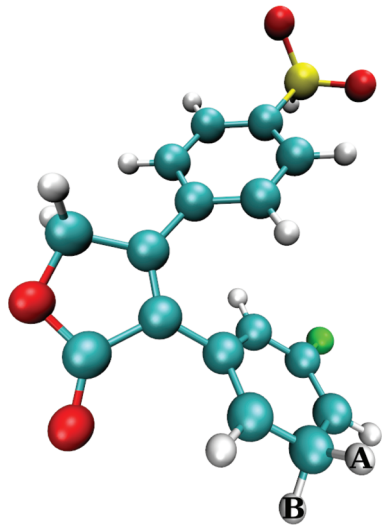

Figure 3. Two orientations for attacks (either side- or face-on) on a nonplanar σ-complex. Molecule shown here is DFU.

predicting epoxidation sites. The results are compiled in Table 1. The data suggest that the hydrogen adducts behave the same way as the methoxy adducts; they fail for the same substrates and give the same success rate of prediction, 83%.

Besides radical adducts, cationic adducts have also been tested initially. Unreasonable gas phase geometries tend to occur when forming adducts using either a hydrogen ion or a methoxy cation, if polar functional groups are present. Applying the solvent continuum can mitigate the problem, but the computation burden increases. A QM/MM study on benzene metabolism by CYP showed that the intermediate adduct has a mixed radical and cationic character,[23] and another study showed that the cationic and radical adducts are in fact close in energy for most substituted benzenes;[6] therefore, we focused our investigation on using radical adduct models for SOM prediction.

When using the thermodynamic stabilities of epoxides to determine the epoxidation sites, the success rate is 83%, which is also excellent. This may be a manifestation of a rather direct epoxide formation from the intermediate and therefore application of the Hammond−Leffler postulate seems to be valid.

Both H- and methoxy-adduct predictions of SOM fail for tolmetin, zomepirac, 1-nitronaphthalene, DPC423, and DPC602. We therefore further examined the individual ring systems of tolmetin, zomepirac, DPC423, and DPC602, as they are larger and more flexible, to check if it was the gas phase QM geometry that caused error in prediction due to an incomplete search of the conformational spaces. We computed each individual aromatic ring of the molecule and calculated the hydrogenation energy for forming the hydrogen adducts, so that we could make direct comparisons among different rings of the same molecule in deciding the favored site. However, using the individual ring systems still failed to predict the experimentally determined sites. It is also possible that the misprediction could originate from the propensity of the system to oxidize aromatic systems through either an electrophilic reaction or a radical reaction path. The pyrazole ring is very electron rich, which makes an electrophilic path more likely. Using a proton probe to mimic that could therefore be of interest. Indeed, the calculated regioselectivity using the proton probe gave the correct site of metabolism by 3.5 kcal/mol for tolmetin. For 1-nitronaphthalene, the proton probe predicts both positions 5 and 10 as

dx.doi.org/10.1021/ci200523f | J. Chem. Inf. Model. 2012, 52, 686−695

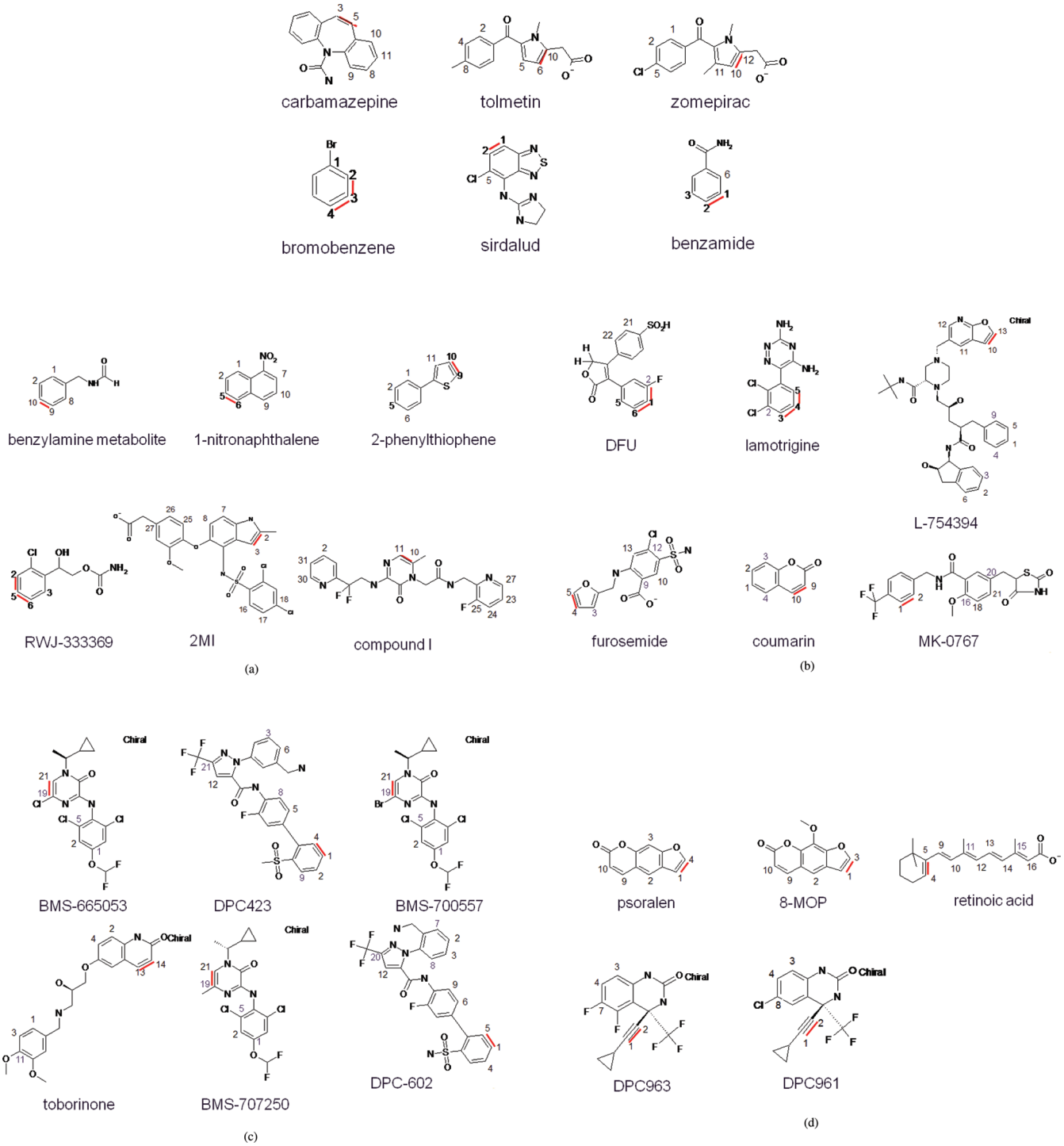

Figure 4. Substrates investigated for epoxide formation sites; bold red lines mark the sites where epoxide forms.

the SOMs, since they differ less than 0.4 kcal/mol in energy (see Supporting Information). These arguments for the prediction failures are not applicable to DPC423 and DPC602. A possible explanation for these two molecules can be that steric effects in the active site of the CYP could influence the site of metabolism for these larger molecules. This is the drawback of the present method. It is conceivable that combining docking of the substances into the relevant CYP isoform protein may improve the site preselection over SASA and hence further enhance the predictive ability. Such studies require experiments to identify the isoform responsible for metabolism.These experiments are relatively complex, and such data are typically not available in early drug discovery programs.

The available experimental data for sites of epoxidation are scarce. In order to extend the chemical diversity for testing the present protocol, we applied it to also predict arene hydroxylation sites. By design, our protocol is not limited to predict only the epoxidation sites; we expected that it can be used for any CYP-mediated reaction that goes via the formation of the σ-intermediate as the rate-determining step. It is widely accepted that epoxidation and hydroxylation occur via a common intermediate when the substrate enters the protein active site.[24] Hence

dx.doi.org/10.1021/ci200523f | J. Chem. Inf. Model. 2012, 52, 686−695

Table 1. Substrates for Predicting Site of Epoxide Formation and the Predictive Performance of Epoxide and Hydrogen Adducts

substrate	predictive ability			no. of possible sites
	epoxide	H-adduct	OMe-adduct	
carbamazepine[27]	√	√	√	7
tolmetin[28]	√	fail	fail	6
zomepirac[28]	√	fail	fail	6
bromobenzene[29]	√	√	√	3
sirdalud[30]	√	√	√	6
benzamide[31]	fail	√	√	3
benzylamine metabolite[31]	fail	√	√	3
1-nitronaphthalene[32]	√	fail	fail	11
2-phenylthiophene[33]	√	√	√	6
RWJ-333369[34,35]	√	√	√	6
2MI[36]	√	√	√	20
thrombin inhibitor compound 1[37]	√	√	√	9
DFU[38]	√	√	√	10
lamotrigine[39]	fail	√	√	6
L-754394[40]	√	√	√	15
furosemide[41]	√	√	√	9
coumarin[42,43]	√	√	√	8
MK-0767[44]	√	√	√	9
BMS-665053[45]	√	√	√	4
DPC423[46]	fail	fail	fail	20
BMS-700557[45]	√	√	√	4
toborinone[47]	√	√	√	13
BMS-707250[45]	√	√	√	4
DPC602[46]	fail	fail	fail	19
psorlen[48]	√	√	√	11
8-MOP[48]	√	√	√	11
retinoic acid[49]	√	√	√	5
DPC963[50]	√	√	√	7
DPC961[51]	√	√	√	7
rank 1 is major	83%	83%	83%	
rank 1 or 2 is major	93%	83%	83%	

Table 2. Substrates for Predicting Site of Hydroxylation and the Predictive Performance of Hydroxide and Hydrogen Adduct

substrate	predictive ability	
	hydroxide	H-adduct
zileuton[52]	√	fail
mexiletine[53,54]	√	√
lidocaine[55]	fail	√
antipyrine[56,57]	fail	√
thiabendazole[58]	fail	fail
imipramine[59]	√	√
propranolol[60,61]	fail	√
cinnarizine[62]	√	√
acenocoumarol[63]	fail	fail
melatonin[64]	√	fail
chlorzoxazone[65]	√	√
propofol[66]	√	fail
o-phenylphenol[67]	fail	fail
galangin[68]	√	√
mephenytoin[69]	√	√
warfarin[70,71]	√	√
ropivacaine[72]	√	√
ropinirole[73]	fail	√
flurbiprofen[74]	√	√
acetanilide[75]	fail	√
bufuralol[76]	√	√
estradiol[77]	√	√
carvedilol[78]	fail	√
7-methoxycoumarin[79]	√	fail
tacrine[80]	fail	√
domperidone[81]	√	fail
aflatoxin[82]	√	√
5-hydroxydiclofenac[83,84]	fail	√
suprofen[85]	fail	√
tienilic acid[86]	fail	√
rank 1 is major/minor	57%	73%
rank 1/2 is major/minor	70%	87%

a method like the present work is well suited for assessing selectivity. We used the stabilization energies of the hydrogen adducts but not the methoxy adducts as the assessment criterion, since both were found to predict equally well in the study of epoxide formation. In addition, the stabilization energies of the hydroxylated products were tested as well.

Predicting the arene hydroxylation is, however, more challenging than the epoxidation site prediction. For the latter case the protocol is considered to give the right answer when either of the two carbon atoms involved is inferred. For the former case of hydroxylation site prediction, the protocol is considered correct only when the exact site is suggested. We also assigned the prediction as a correct one when the prediction corresponds to a minor SOM that is reported in the literature, and in fact, this extension has only been applied to mexiletine. Nevertheless, the predictive ability of using the hydrogen adduct is still above 70% (see Table 2) from a set of 30 substrates shown in Figure 5. However, the predictive ability by comparing the energies of hydroxylated products is rather low: just above 50%. This implies that many hydroxylated products bear less resemblance to the structures of the transition state forming the σ-intermediate, due to, e.g., a multiple-step mechanism or the existence of more than one reaction path. It is known that, in addition to a direct conversion via the proton-shuttle mechanism or through an NIH shift (the migration of the hydrogen from the site of hydroxylation to the adjacent carbon[25]) and a keto−enol tautomerization, arene hydroxylation can also occur via an epoxide intermediate.[4,25,26]

Dividing the structure into its constituting ring systems was also tested out for failed cases of hydroxylation when using the adduct model on a more flexible substrate. However, the same results were obtained for both acenocoumarol and domperidone. For *o*-phenylphenol, QM still failed to favor the para-position to the hydroxy group in either the *o*-methylphenol or the phenol model.

By analyzing the results obtained in this work we assess if our assumptions and simplifications give rise to potential errors in site prediction:

(1) Geometry optimization was performed in gas phase, with solvation energy correction added for the final structure. For most of the cases, the energy rankings are unchanged comparing the gas phase energies to the solvation-corrected single point energies. If the rankings differed, then we performed optimization with solvation effects included. Such resultant rankings are often the same as

dx.doi.org/10.1021/ci200523f | J. Chem. Inf. Model. 2012, 52, 686−695

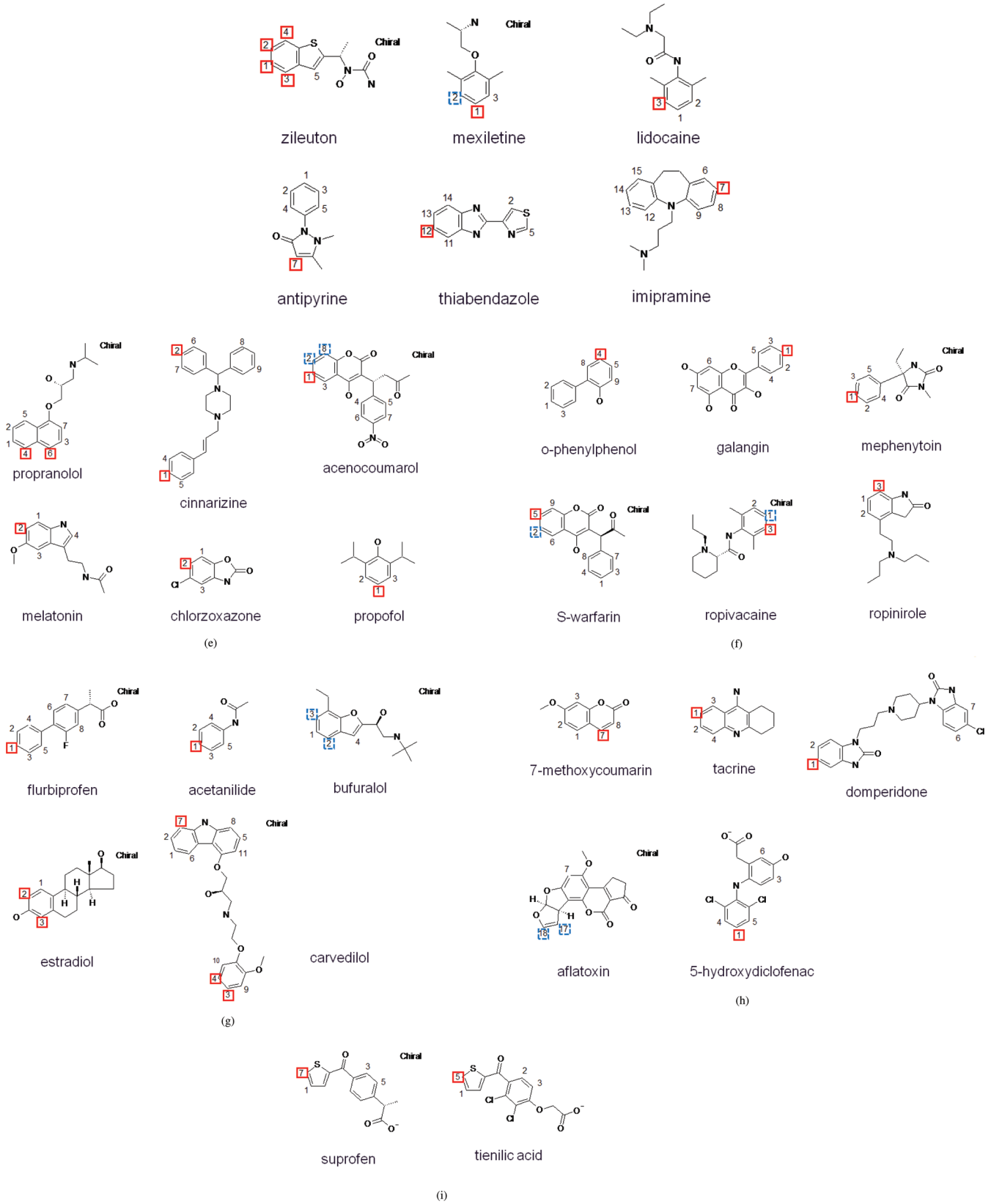

Figure 5. Substrates investigated for hydroxylation sites; bold red squares indicate the major metabolic sites, while dashed blue squares indicate the minor sites.

those by adding the solvation correction at the end, indicating that this latter simplification is adequate. Moreover, the energy differences among those sites in question are rather small (<1 kcal/mol). Molecules with such inconsistency are the hydrogen adducts of zileuton, lidocaine, estradiol, and 5-OH-diclofenac. The hydroxides of zileuton, the epoxides of 1-nitronaphthalene, and the methoxy adducts of retinoic acid also show this finding.

dx.doi.org/10.1021/ci200523f | J. Chem. Inf. Model. 2012, 52, 686–695

(2) The conformation in the real protein binding mode was ignored, only the electronic reactivity was considered. In order to include the conformation information, the main CYP isoform that is responsible for metabolizing the substrate needs to be identified. Furthermore, the crystal structure has to be available to apply docking methodology. Without the binding site-specific information, our method gave a high success rate in SOM prediction and fulfilled the purpose of this study, namely to reliably and practically identify SOM. A similar observation has been made by obtaining the same predicting ability using a substrate−property based method, compared to that using a combined method with both substrate property and docking,[10] thus the molecular properties of the substrates seem most important in metabolism.

(3) Modeling the iron-oxo porphyrin moiety with a methoxy or a hydrogen radical. The correlation of activation energies calculated using surrogate adducts and full model has been found to be 79%[15], as mentioned above. The outcomes of the present study also confirm that the use of surrogate adducts leads to fair success in epoxidation as well as hydroxylation site predictions, 83% and 73%, respectively. The further simplification of using a hydrogen atom to replace methoxy radical performs well and does not introduce additional error. The two protocols gave identical predicting performance. However, the nonperfect correlation between the surrogate and iron-oxo porphyrin models itself implies one source of error in using our protocol.

(4) Using the Hammond−Leffler postulate, assuming that the natures of the transition state and the adduct intermediate or the product (epoxide or hydroxide) are alike. Judging from our results, this assumption appears sound for using an adduct intermediate to depict the closely related transition state. By using the product, it seems that the epoxide still resembles the transition state, while the hydroxide does not. This agrees with the findings that there are several formation pathways for the hydroxide, while the conversion from the transition state to epoxide is rather straightforward.

The accuracy of the protocol using a model intermediate, i.e., the adduct formation, for epoxidation is not improved by counting both of the predicted top two sites as possible major metabolic sites, owing to the fact that we used SASA to pick the most sterically probable metabolic sites. In those failed cases, the assignments made by using SASA followed by QM calculations indicated the wrong aromatic ring compared with the experimentally determined one with respect to the SOM. Still, the method produced 83% correct first-ranked assignments and the experimental metabolites are almost always among the preselected sites, except for two cases where there are multiple sites of hydroxylation (zileuton and bufuralol). If we count that either the predicted rank 1 or 2 SOM is a major metabolite as successful, then the predictive ability of using the epoxide probe increases to 93%. For hydroxylation, such counting increases the success rate of using the hydroxide and the hydrogen adduct to 70% and 87%, respectively. The results presented in this work for predicting the site of epoxide formation and hydroxylation, respectively, are both well above 80%. However, taking into account the many possible sites of attack for each system (compound), e.g., 15 sites for compound L-754394 (see Table 1 for a list of number of sites), the results are more precise than simply indicated by accuracy based on a correct/incorrect estimate for each particular compound. Considering all the possible atoms that potentially could be the SOM, there are 238 such points of attack for the structures studied in this work. With this in mind, 5 erroneous predictions (97.8% correctness) indicate that the approach put forward in this work seems to be a rather predictive approach for assigning the correct SOM to compounds that may undergo epoxide formation or hydroxylation.

Since the aim of the present work is to correctly, yet pragmatically, predict the epoxidation sites in order to address reactive metabolite formation, we limited our calculations to carbon atoms. However, in contrast to rule-based methods, this protocol can be used to study the oxidation of heteroatoms directly with a few modifications in selecting atoms to be studied, since there is no need for parametrization or rule making, but straightforward DFT calculations on model systems.

■ CONCLUSION

The present protocol uses DFT calculations to determine SOMs, and the time frame is in terms of minutes to hours and, therefore, well within the typical design−make−test cycle of drug discovery. In contrast to the widely applied rule-based methods for the SOM prediction, our approach employs straightforward DFT calculations for energy comparisons, hence avoids rule derivation, trend fitting, and the need of any training sets. DFT calculations are performed for energy minima search on model σ-intermediates instead of searching for the transition states of the full model of the CYP−substrate complex. Therefore it is possible to take advantage of the accuracy of DFT and yet remain affordable with respect to computational considerations.

All probes, i.e., epoxide, hydrogen adduct, and methoxy adduct as the model σ-intermediate, have a similar success rate in predicting the first-ranked site of epoxidation. Among them, the hydrogen adduct probe is the most efficient because it does not produce more than one conformation and thus requires the least number of calculations per molecule.

When extending the application of this method to further test its usefulness by studying sites of hydroxylation, the success rate of using hydroxide as the probe is rather poor, while using the hydrogen adduct gives comparable predictive performance to that of the epoxidation study. The present method with surrogate σ-intermediate is thus applicable in predicting CYP-mediated epoxidation and hydroxylation reactions where the rate-determining step is the formation of the σ-intermediate. Though a ligand-based approach could be improved by the addition of more realistic substrate poses in the enzyme using, e.g., docking procedure, the present protocol was able to give around 80% successful prediction.

■ ASSOCIATED CONTENT

Supporting Information

Detailed information of all substrates, SASA, ranks, and energies of selected carbon sites.

This material is available free of charge via the Internet at http://pubs.acs.org.

■ AUTHOR INFORMATION

Corresponding Author

*E-mail: ulf.norinder@astrazeneca.com.

Notes

The authors declare no competing financial interest.

REFERENCES

(1) Thompson, R. A.; Isin, E. M.; Li, Y.; Weaver, R.; Weidolf, L.; Wilson, I.; Claesson, A.; Page, K.; Dolgos, H.; Kenna, J. G. Risk Assessment and Mitigation Strategies for Reactive Metabolites in Drug Discovery and Development. *Chem.-Biol. Interact.* **2011**, *192*, 65−71.

(2) Prakash, C.; Sharma, R.; Gleave, M.; Nedderman, A. In Vitro Screening Techniques for Reactive Metabolites for Minimizing Bioactivation Potential in Drug Discovery. *Curr. Drug. Metab.* **2008**, *9*, 952−964.

(3) Walsh, J. S.; Miwa, G. T. Bioactivation of Drugs: Risk and Drug Design. *Annu. Rev. Pharmacol. Toxicol.* **2011**, *51*, 145−167.

(4) Korzekwa, K. R.; Swinney, D. C.; Trager, W. F. Isotopically Labeled Chlorobenzenes as Probes for the Mechanism of Cytochrome P-450 Catalyzed Aromatic Hydroxylation. *Biochemistry* **1989**, *28*, 9019−9027.

(5) Jones, J. P.; Mysinger, M.; Korzekwa, K. R. Computational Models for Cytochrome P450: A Predictive Electronic Model for Aromatic Oxidation and Hydrogen Atom Abstraction. *Drug Metab. Dispos.* **2002**, *30*, 7−12.

(6) Bathelt, C. M.; Ridder, L.; Mulholland, A. J.; Harvey, J. N. Mechanism and Structure-Reactivity Relationships for Aromatic Hydroxylation by Cytochrome P450. *Org. Biomol. Chem.* **2004**, *2*, 2998−3005.

(7) Tarcsay, Á.; Keserü, G. M. In Silico Site of Metabolism Prediction of Cytochrome P450-Mediated Biotransformations. *Expert. Opin. Metab. Toxicol.* **2011**, *7*, 299−312.

(8) Leffler, J. E. Parameters for the Description of Transition States. *Science* **1953**, *117*, 340−341.

(9) Hammond, G. S. A Correlation of Reaction Rates. *J. Am. Chem. Soc.* **1955**, *77*, 334−338.

(10) Rydberg, P.; Vasanthanathan, P.; Oostenbrink, C.; Olsen, L. Fast Prediction of Cytochrome P450 Mediated Drug Metabolism. *Chem. Med. Chem.* **2009**, *4*, 2070−2079.

(11) Lee, B.; Richards, F. M. The Interpretation of Protein Structures: Estimation of Static Accessibility. *J. Mol. Biol.* **1971**, *55*, 379−400.

(12) The CCP4 Suite: Programs for Protein Crystallography. *Acta Cryst. D* **1994**, *50*, 760-763, Collaborative Computational Project, Number 4, 1994.

(13) Ogliaro, F.; Filatov, M.; Shaik, S. Alkane Hydroxylation by Cytochrome P450: Is Kinetic Isotope Effect a Reliable Probe of Transition State Structure? *Eur. J. Inorg. Chem.* **2000**, *12*, 2455−2458.

(14) Olsen, L.; Rydberg, P.; Rod, T. H.; Ryde, U. Prediction of Activation Energies for Hydrogen Abstraction by Cytochrome P450. *J. Med. Chem.* **2006**, *49*, 6489−6499.

(15) Rydberg, P.; Ryde, U.; Olsen, L. Prediction of Activation Energies for Aromatic Oxidation by Cytochrome P450. *J. Phys. Chem. A* **2008**, *112*, 13058−13065.

(16) Frisch, J.; Trucks, G. W.; Schlegel, H. B.; Scuseria, G. E.; Robb, M. A.; Cheeseman, J. R.; Scalmani, G.; Barone, V.; Mennucci, B.; Petersson, G. A.; Nakatsuji, H.; Caricato, M.; Li, X.; Hratchian, H. P.; Izmaylov, A. F.; Bloino, J.; Zheng, G.; Sonnenberg, J. L.; Hada, M.; Ehara, M.; Toyota, K.; Fukuda, R.; Hasegawa, J.; Ishida, M.; Nakajima, T.; Honda, Y.; Kitao, O.; Nakai, H.; Vreven, T.; Montgomery, J. A., Jr.; Peralta, J. E.; Ogliaro, F.; Bearpark, M.; Heyd, J. J.; Brothers, E.; Kudin, K. N.; Staroverov, V. N.; Kobayashi, R.; Normand, J.; Raghavachari, K.; Rendell, A.; Burant, J. C.; Iyengar, S. S.; Tomasi, J.; Cossi, M.; Rega, N.; Millam, J. M.; Klene, M.; Knox, J. E.; Cross, J. B.; Bakken, V.; Adamo, C.; Jaramillo, J.; Gomperts, R.; Stratmann, R. E.; Yazyev, O.; Austin, A. J.; Cammi, R.; Pomelli, C.; Ochterski, J. W.; Martin, R. L.; Morokuma, K.; Zakrzewski, V. G.; Voth, G. A.; Salvador, P.; Dannenberg, J. J.; Dapprich, S.; Daniels, A. D.; Farkas, Ö.; Foresman, J. B.; Ortiz, J. V.; Cioslowski, J.; Fox, D. J. *Gaussian 09*, revision A.1; Gaussian Inc.: Wallingford, CT, 2009.

(17) Becke, A. D. Density-Functional Thermochemistry. III. The Role of Exact Exchange. *J. Chem. Phys.* **1993**, *98*, 5648−5652.

(18) Lee, C.; Yang, W.; Parr, R. G. Development of the Colle-Salvetti Correlation-Energy Formula into a Functional of the Electron Density. *Phys. Rev. B* **1988**, *37*, 785−789.

(19) Hehre, W. J.; Ditchfield, R.; Pople, J. A. Self-Consistent Molecular Orbital Methods. 12. Further Extensions of Gaussian-Type Basis Sets for Use in Molecular-Orbital Studies of Organic-Molecules. *J. Chem. Phys.* **1972**, *56*, 2257−2261.

(20) Hariharan, P. C.; Pople, J. A. Influence of Polarization Functions on Molecular-Orbital Hydrogenation Energies. *Theor. Chem. Acc.* **1973**, *28*, 213−222.

(21) Francl, M. M.; Pietro, W. J.; Hehre, W. J.; Binkley, J. S.; Defrees, D. J.; Pople, J. A.; Gordon, M. S. Self-Consistent Molecular Orbital Methods. 23. A Polarization-Type Basis Set for 2nd-Row Elements. *J. Chem. Phys.* **1982**, *77*, 3654−3665.

(22) Tomasi, J.; Mennucci, B.; Cammi, R. Quantum Mechanical Continuum Solvation Models. *Chem. Rev.* **2005**, *105*, 2999−3093.

(23) Bathelt, C. M.; Mulholland, A. J.; Harvey, J. N. QM/MM Modeling of Benzene Hydroxylation in Human Cytochrome P450 2C9. *J. Phys. Chem. A* **2008**, *112*, 13149−13156.

(24) Denisov, I.; Makris, T.; Sligar, S.; Schlichting, I. Structure and Chemistry of Cytochrome P450. *Chem. Rev.* **2005**, *105*, 2253−2278.

(25) Guroff, G.; Daly, J. W.; Jerina, D. M.; Renson, J.; Witkop, B.; Undenfriend, S. Hydroxylation-Induced Migration: The NIH Shift. *Science* **1967**, *157*, 1524−1530.

(26) Jerina, D. M.; Daly, J. W.; Witkop, B.; Zaltzman-Nirenberg, P.; Undenfriend, S. The Role of Arene Oxide-oxepin Systems in the Metabolism of Aromatic Substrates. III. Formation of 1,2-Naphthalene Oxide from Naphthalene by Liver Microsomes. *J. Am. Chem. Soc.* **1968**, *90*, 6525−6527.

(27) Bu, H.; Kang, P.; Deese, A.; Zhao, P.; Pool, W. Human in Vitro Glutathionyl and Protein Adducts of Carbamazepine-10,11-Epoxide, a Stable and Pharmacologically Active Metabolite of Carbamazepine. *Drug Metab. Dispos.* **2005**, *33*, 1920−1924.

(28) Chen, Q.; Doss, G.; Tung, E.; Liu, W.; Tang, Y.; Braun, M.; Didolkar, V.; Strauss, J.; Wang, R.; Stearns, R.; Evans, D.; Baillie, T.; Tang, W. Evidence for the Bioactivation of Zomepirac and Tolmetin by an Oxidative Pathway: Identification of Glutathione Adducts in Vitro in Human Liver Microsomes and in Vivo in Rats. *Drug Metab. Dispos.* **2006**, *34*, 145−151.

(29) Zheng, J.; Hanzlik, R. Premercapturic Acid Metabolites of Bromobenzene Derived via Its 2,3-Oxide and 3,4-Oxide Metabolites. *Xenobiotica* **1991**, *21*, 535−546.

(30) Koch, P.; Hirst, D.; von Wartburg, B. Biological Fate of Sirdalud in Animals and Man. *Xenobiotica* **1989**, *19*, 1255−1265.

(31) Mutlib, A.; Dickenson, P.; Chen, S.; Espina, R.; Daniels, J.; Gan, L. Bioactivation of Benzylamine to Reactive Intermediates in Rodents: Formation of Glutathione, Glutamate, and Peptide Conjugates. *Chem. Res. Toxicol.* **2002**, *15*, 1190−1207.

(32) Watt, K.; Morin, D.; Kurth, M.; Mercer, R.; Plopper, C.; Buckpitt, A. Glutathione Conjugation of Electrophilic Metabolites of 1-Nitronaphthalene in Rat Tracheobronchial Airways and Liver: Identification by Mass Spectrometry and Proton Nuclear Magnetic Resonance Spectroscopy. *Chem. Res. Toxicol.* **1999**, *12*, 831−839.

(33) Dansette, P. M.; Bertho, G.; Mansuy, D. First Evidence that Cytochrome P450 May Catalyze both S-Oxidation and Epoxidation of Thiophene Derivatives. *Biochem. Biophys. Res. Commun.* **2005**, *338*, 450−455.

(34) Mannens, G. S. J.; Hendrickx, J.; Janssen, C. G. M.; Chien, S.; Van Hoof, B.; Verhaeghe, T.; Kao, M.; Kelley, M. F.; Goris, I.; Bockx, M.; Verreet, B.; Bialer, M.; Meuldermans, W. The Absorption, Metabolism, and Excretion of the Novel Neuromodulator RWJ-333369 (1,2-Ethanediol, [1−2-Chlorophenyl]-, 2-Carbamate, [S]-) in Humans. *Drug Metab. Dispos.* **2007**, *35*, 554−565.

(35) Mamidi, R. N. V. S.; Mannens, G.; Annaert, P.; Hendrickx, J.; Goris, I.; Bockx, M.; Janssen, C. G. M.; Kao, M.; Kelley, M. F.; Meuldermans, W. Metabolism and Excretion of RWJ-333369 [1,2-Ethanediol, 1-(2-Chlorophenyl)-, 2-Carbamate, (S)-] in Mice, Rats, Rabbits, and Dogs. *Drug Metab. Dispos.* **2007**, *35*, 566−575.

(36) Wong, S. G.; Fan, P. W.; Subramanian, R.; Tonn, G. R.; Henne, K. R.; Johnson, M. G.; Lohr, M. T.; Wong, B. K. Bioactivation of a Novel 2-Methylindole-Containing Dual Chemoattractant Receptor-Homologous Molecule Expressed on T-Helper Type-2 Cells/D-Prostanoid Receptor

Antagonist Leads to Mechanism-Based CYP3A Inactivation: Glutathione Adduct Characterization and Prediction of In Vivo Drug-Drug Interaction. *Drug Metab. Dispos.* **2010**, *38*, 841−850.
(37) Singh, R.; Elipe, M. V. S.; Pearson, P. G.; Arison, B. H.; Wong, B. K.; White, R.; Yu, X.; Burgey, C. S.; Lin, J. H.; Baillie, T. A. Metabolic Activation of a Pyrazinone-Containing Thrombin Inhibitor. Evidence for Novel Biotransformation Involving Pyrazinone Ring Oxidation, Rearrangement, and Covalent Binding to Proteins. *Chem. Res. Toxicol.* **2003**, *16*, 198−207.
(38) Yergey, J. A.; Trimble, L. A.; Silva, J.; Chauret, N.; Li, C.; Therien, M.; Grimm, E.; Nicoll-Griffith, D. A. In Vitro Metabolism of the COX-2 Inhibitor DFU, Including a Novel Glutathione Adduct Rearomatizationa. *Drug Metab. Dispos.* **2001**, *29*, 638−644.
(39) Chen, H.; Grover, S.; Yu, L.; Walker, G.; Mutlib, A. Bioactivation of Lamotrigine in Vivo in Rat and in Vitro in Human Liver Microsomes, Hepatocytes, and Epidermal Keratinocytes: Characterization of Thioether Conjugates by Liquid Chromatography/Mass Spectrometry and High Field Nuclear Magnetic Resonance Spectroscopy. *Chem. Res. Toxicol.* **2010**, *23*, 159−170.
(40) SahaliSahly, Y.; Balani, S. K.; Lin, J. H.; Baillie, T. A. In Vitro Studies on the Metabolic Activation of the Furanopyridine L-754,394, a Highly Potent and Selective Mechanism-Based Inhibitor of Cytochrome P450 3A4. *Chem. Res. Toxicol.* **1996**, *9*, 1007−1012.
(41) Williams, D. P.; Antoine, D. J.; Butler, P. J.; Jones, R.; Randle, L.; Payne, A.; Howard, M.; Gardner, I.; Blagg, J.; Park, B. K. The Metabolism and Toxicity of Furosemide in the Wistar Rat and CD-1 Mouse: a Chemical and Biochemical Definition of the Toxicophore. *J. Pharmacol. Exp. Ther.* **2007**, *322*, 1208−1220.
(42) Born, S. L.; Rodriguez, P. A.; Eddy, C. L.; LehmanMcKeeman, L. D. Synthesis and Reactivity of Coumarin 3,4-Epoxide. *Drug Metab. Dispos.* **1997**, *25*, 1318−1323.
(43) Born, S. L.; Caudill, D.; Fliter, K. L.; Purdon, M. P. Identification of the Cytochromes P450 that Catalyze Coumarin 3,4-Epoxidation and 3-Hydroxylation. *Drug Metab. Dispos.* **2002**, *30*, 483−487.
(44) Reddy, V.; Doss, G.; Creighton, M.; Kochansky, C.; Vincent, S.; Franklin, R.; Karanam, B. Identification and Metabolism of a Novel Dihydrohydroxy-S-glutathionyl Conjugate of a Peroxisome Proliferator-activated Receptor Agonist, MK-0767 [(±)-5-[(2,4-dioxothiazolidin-5-yl)methyl]-2-methoxy-N-[[(4-tr ifluoromethyl)phenyl]methyl] enzamide], in Rats. *Drug Metab. Dispos.* **2004**, *32*, 1154−1161.
(45) Zhuo, X.; Hartz, R. A.; Bronson, J. J.; Wong, H.; Ahuja, V. T.; Vrudhula, V. M.; Leet, J. E.; Huang, S.; Macor, J. E.; Shu, Y.-Z. Comparative Biotransformation of Pyrazinone-Containing Corticotropin-Releasing Factor Receptor-1 Antagonists: Minimizing the Reactive Metabolite Formation. *Drug Metab. Dispos.* **2010**, *38*, 5−15.
(46) Mutlib, A. E.; Shockcor, J.; Chen, S. Y.; Espina, R. J.; Pinto, D. J.; Orwat, M. J.; Prakash, S. R.; Gant, L. S. Disposition of 1-[3-(Aminomethyl)phenyl]-N-[3-fluoro-2′(methylsulfonyl)-[1,1″- biphenyl]-4-yl]-3-(trifluoromethyl)-1H-Pyrazole-5-Carboxamide (DPC 423) by Novel Metabolic Pathways. Characterization of Unusual Metabolites by liquid Chromatography/Mass Spectrometry and NMR. *Chem. Res. Toxicol.* **2002**, *15*, 48−62.
(47) Kitani, M.; Miyamoto, G.; Nagasawa, M.; Yamada, T.; Matsubara, J.; Uchida, M.; Odomi, M. Biotransformation of the Novel Inotropic Agent Toborinone (OPC-18790) in Rats and Dogs - Evidence for the Formation of Novel Glutathione and Two Cysteine Conjugates. *Drug Metab. Dispos.* **1997**, *25*, 663−674.
(48) Koenigs, L. L.; Trager, W. F. Mechanism-Based Inactivation of Cytochrome P450 2B1 by 8-Methoxypsoralen and Several Other Furanocoumarins. *Biochemistry* **1998**, *37*, 13184−13193.
(49) McCormick, A. M.; Napoli, J. L.; Schnoes, H. K.; Deluca, H. F. Isolation and Identification of 5,6-Epoxyretinoic Acid - Biologically-Active Metabolite of Retinoic Acid. *Biochemistry* **1978**, *17*, 4085−4090.
(50) Chen, H.; Shockcor, J.; Chen, W.; Espina, R.; Gan, L.-S.; Mutlib, A. E. Delineating Novel Metabolic Pathways of DPC 963, a Non-Nucleoside Reverse Transcriptase Inhibitor, in Rats. Characterization of Glutathione Conjugates of Postulated Oxirene and Benzoquinone Imine Intermediates by LC/MS and LC/NMR. *Chem. Res. Toxicol.* **2002**, *15*, 388−399.
(51) Mutlib, A.; Chen, H.; Shockcor, J.; Espina, R.; Chen, S.; Cao, K.; Du, A.; Nemeth, G.; Prakash, S.; Gan, L.-S. Characterization of Novel Glutathione Adducts of a Non-Nucleoside Reverse Transcriptase Inhibitor, (S)-6-Chloro-4-(cyclopropylethynyl)-4-(trifluoromethyl)-3,4-dihydro-2(1H)-quinazolinone (DPC 961), in Rats. Possible Formation of an Oxirene Metabolic Intermediate from a Disubstituted Alkyne. *Chem. Res. Toxicol.* **2000**, *13*, 775−784.
(52) Machinist, J. M.; Mayer, M. D.; Shet, M. S.; Ferrero, J. L.; Rodrigues, A. D. Identification of the Human Liver Cytochrome-P450 Enzymes Involved in the Metabolism of Zileuton (ABT-077) and ITS N-Dehydroxylated Metabolite, ABBOTT-66193. *Drug Metab. Dispos.* **1995**, *23*, 1163−1174.
(53) Turgeon, J.; Fiset, C.; Giguere, R.; Gilbert, M.; Moerike, K.; Rouleau, J. R.; Kroemer, H. K.; Eichelbaum, M.; Grechbelanger, O.; Belanger, P. M. Influence of Debrisoquine Phenotype and of Quinidine on Mexiletine Disposition in Man. *J. Pharmacol. Exp. Ther.* **1991**, *259*, 789−798.
(54) Nakajima, M.; Kobayashi, K.; Shimada, N.; Tokudome, S.; Yamamoto, T.; Kuroiwa, Y. Involvement of CYPIA2 in Mexiletine Metabolism. *Br. J. Clin. Pharmacol.* **1998**, *46*, 55−62.
(55) Imaoka, S.; Enomoto, K.; ODA, Y.; Asada, A.; Fujimori, M.; Shimada, T.; Fujita, S.; Guengerich, F. P.; Funae, Y. Lidocaine Metabolism by Human Cytochrome-P-450s Pirified from Hepatic Microsomes - Comparison of Those with Rar Hepatic Cytochrome-P-450s. *J. Pharmacol. Exp. Ther.* **1990**, *255*, 1385−1391.
(56) Matzke, G.; Frye, R.; Early, J.; Straka, R.; Carson, S. Evaluation of the Influence of Diabetes Mellitus on Antipyrine Metabolism and CYP1A2 and CYP2D6 Activity. *Pharmacotherapy* **2000**, *20*, 182−190.
(57) Engel, G.; Hofmann, U.; Heidemann, H.; Cosme, J.; Eichelbaum, M. Antipyrine as a Probe for Human Oxidative Drug Metabolism: Identification of the Cytochrome P450 Enzymes Catalyzing 4-Hydroxyantipyrine, 3-Hydromethylantipyrine, and Norantipyrine Formation. *Clin. Pharmacol. Ther.* **1996**, *59*, 613−623.
(58) Coulet, M.; Dacasto, M.; Eeckhoutte, C.; Larrieu, G.; Sutra, J.; Alvinerie, M.; Mace, K.; Pfeifer, A.; Galtier, P. Identification of Human and Rabbit Cytochromes P450 1A2 as Major Isoforms Involved in Thiabendazole 5-Hydroxylation. *Fundam. Clin. Pharmacol.* **1998**, *12*, 225−235.
(59) Koyama, E.; Chiba, K.; Tani, M.; Ishizaki, T. Reappraisal of Human CYP Isoforms Involved in Imipramine N-Demethylation and 2-Hydroxylation: A Study using Microsomes Obtained from Putative Extensive and Poor Metabolizers of S-Mephenytoin and Eleven Recombinant Human CYPs. *J. Pharmacol. Exp. Ther.* **1997**, *281*, 1199−1210.
(60) Ching, M. S.; Bichara, N.; Blake, C. L.; Ghabrial, H.; Tukey, R. H.; Smallwood, R. A. Propranolol 4- and 5-Hydroxylation and N-Desisopropylation by Cloned Human Cytochrome P4501A1 and P4501A2. *Drug Metab. Dispos.* **1996**, *24*, 692−694.
(61) Masubuchi, Y.; Hosokawa, S.; Horie, T.; Suzuki, T.; Ohmori, S.; Kitada, M.; Narimatsu, S. Cytochrome-P450 Isozymes Involved in Propranolol Metabolism in Human Liver-Microsomes - The Role of CYP2D6 as Ring-Hydroxylase and CYP1A2 as N-Desisopropylase. *Drug Metab. Dispos.* **1994**, *22*, 909−915.
(62) Kariya, S.; Isozaki, S.; Uchino, K.; Suzuki, T.; Narimatsu, S. Oxidative Metabolism of Flunarizine and Cinnarizine by Microsomes from B-Lymphoblastoid Cell Lines Expressing Human Cytochrome P450 Enzymes. *Biol. Pharmacol. Bull.* **1996**, *19*, 1511−1514.
(63) Thijssen, H.; Flinois, J.; Beaune, P. Cytochrome P4502C9 is the Principal Catalyst of Racemic Acenocoumarol Hydroxylation Reactions in Human Liver Microsomes. *Drug Metab. Dispos.* **2000**, *28*, 1284−1290.
(64) Ma, X. C.; Idle, J. R.; Krausz, K. W.; Gonzalez, F. Metabolism of Melatonin by Human Cytochromes P450. *Drug Metab. Dispos.* **2005**, *33*, 489−494.
(65) Shimada, T.; Tsumura, F.; Yamazaki, H. Prediction of Human Liver Microsomal Oxidations of 7-Ethoxycoumarin and Chlorzoxazone

with Kinetic Parameters of Recombinant Cytochrome P-450 Enzymes. *Drug Metab. Dispos.* **1999**, *27*, 1274−1280.
(66) Guitton, J.; Buronfosse, T.; Desage, M.; Flinois, J. P.; Perdrix, J. P.; Brazier, J. L.; Beaune, P. Possible Involvement of Multiple Human Cytochrome P450 Isoforms in the Liver Metabolism of Propofol. *Brit. J. Anaesth.* **1998**, *80*, 788−795.
(67) Ozawa, S.; Ohta, K.; Miyajima, A.; Kurebayashi, H.; Sunouchi, M.; Shimizu, M.; Murayama, N.; Matsumoto, Y.; Fukuoka, M.; Ohno, Y. Metabolic Activation of O-Phenylphenol to a Major Cytotoxic Metabolite, Phenylhydroquinone: Role of Human CYP1A2 and Rat CYP2C11/CYP2E1. *Xenobiotica* **2000**, *30*, 1005−1017.
(68) Otake, Y.; Walle, T. Oxidation of the Flavonoids Galangin and Kaempferide by Human Liver Microsomes and CYP1A1, CYP1A2, and CYP2C9. *Drug Metab. Dispos.* **2002**, *30*, 103−105.
(69) Coller, J. K.; Somogyi, A. A.; Bochner, F. Comparison of (S)-Mephenytoin and Proguanil Oxidation in Vitro: Contribution of Several CYP Isoforms. *Br. J. Clin. Pharmacol.* **1999**, *48*, 158−167.
(70) Rettie, A. E.; Korzekwa, K. R.; Kunze, K. L.; Lawrence, R. F.; Eddy, A. C.; Aoyama, T.; Gelboin, H. V.; Gonzalez, F. J.; Trager, W. F. Hydroxylation of Warfarin by Human cDNA-Expressed Cytochrome-P-450 - A Role for P-4502C9 in the Etiology of (S)-Warfarin DRUG-Interactions. *Chem. Res. Toxicol.* **1992**, *5*, 54.
(71) Zhang, Z.; Fasco, M.; Huang, Z.; Guengerich, F.; Kaminsky, L. Human Cytochromes P4501A1 and P4501A2: R-Warfarin Metabolism as a Probe. *Drug Metab. Dispos.* **1995**, *23*, 1339−1345.
(72) Ekström, G.; Gunnarsson, U. Ropivacaine, a New Amide-Type Local Anesthetic Agent, is Metabolized by Cytochromes P450 1A and 3A in Human Liver Microsomes. *Drug Metab. Dispos.* **1996**, *24*, 955−961.
(73) Bloomer, J.; Clarke, S.; Chenery, R. In Vitro Identification of the P450 Enzymes Responsible for the Metabolism of Ropinirole. *Drug Metab. Dispos.* **1997**, *25*, 840−844.
(74) Tracy, T. S.; Rosenbluth, B. W.; Wrighton, S. A.; Gonzalez, F. J.; Korzekwa, K. R. Role of Cytochrome-P450 2C9 and an Allelic Variant in the 4′-Hydroxylation of (R)-Flurbiprofen and (S)-Flurbiprofen. *Biochem. Pharmacol.* **1995**, *49*, 1269−1275.
(75) Liu, G.; Gelboin, H. V.; Myers, M. J. Role of Cytochrome P450 IA2 in Acetanilide 4-Hydroxylation as Determined with cDNA Expression and Monoclonal Antibodies. *Arch. Biochem. Biophys.* **1991**, *284* (2), 400−406.
(76) Yamazaki, H.; Guo, Z.; Persmark, M.; Mimura, M.; Inoue, K.; Guengerich, F.; Shimada, T. Bufuralol Hydroxylation by Cytochrome-P450 2D6 AND 1A2 Enzymes in Human Liver-Microsomes. *Mol. Pharmacol.* **1994**, *46*, 568−577.
(77) Yamazaki, H.; Inoue, K.; Shaw, P.; Checovich, W. J.; Guengerich, F.; Shimada, T. Different Contributions of Cytochrome P450 2C19 and 3A4 in the Oxidation of Omeprazole by Human Liver Microsomes: Effects of Contents of These Two Forms in Individual Human Samples. *J. Pharmacol. Exp. Ther.* **1997**, *283*, 434−442.
(78) Oldham, H. G.; Clarke, S. E. In Vitro Identification of the Human Cytochrome P450 Enzymes Involved in the Metabolism of R(+)- and S(-)-Carvedilol. *Drug Metab. Dispos.* **1997**, *25*, 970−977.
(79) Kim, K.; Isin, E.; Yun, C.; Kim, D.; Guengerich, F. Kinetic Deuterium Isotope Effects for 7-Alkoxycoumarin O-Dealkylation Reactions Catalyzed by Human Cytochromes P450 and in Liver Microsomes - Rate-Limiting C-H Bond Breaking in Cytochrome P450 1A2 Substrate Oxidation. *FEBS J.* **2006**, *273*, 2223−2231.
(80) Spaldin, V.; Madden, S.; Adams, D. A.; Edwards, R. J.; Davies, D. S.; Park, B. K. Determination of Human Hepatic Cytochrome P4501A2 Activity in-Vitro - Use of Tacrine as an Isoenzyme-Specific Probe. *Drug Metab. Dispos.* **1995**, *23*, 929−934.
(81) Ward, B. A.; Morocho, A.; Kandil, A.; Galinsky, R. E.; Flockhart, D. A.; Desta, Z. Characterization of Human Cytochrome P450 Enzymes Catalyzing Domperidone N-Dealkylation and Hydroxylation in Vitro. *Br. J. Clin. Pharmacol.* **2004**, *58*, 277−287.
(82) He, X.; Tang, L.; Wang, S.; Cai, Q.; Wang, J.; Hong, J. Efficient Activation of Aflatoxin B-1 by Cytochrome P450 2A13, an Enzyme Predominantly Expressed in Human Respiratory Tract. *Int. J. Cancer* **2006**, *118*, 2665−2671.
(83) Mancy, A.; Antignac, M.; Minoletti, C.; Dijols, S.; Mouries, V.; Duong, N. T. H.; Battioni, P.; Dansette, P. M.; Mansuy, D. Diclofenac and its Derivatives as Tools for Studying Human Cytochromes P450 Active Sites: Particular Efficiency and Regioselectivity of P4502Cs. *Biochemistry* **1999**, *38*, 14264−14270.
(84) Bort, R.; Mace, K.; Boobis, A.; Gomez-Lechon, M. J.; Pfeifer, A.; Castell, J. Hepatic Metabolism of Diclofenac: Role of Human CYP in the Minor Oxidative Pathways. *Biochem. Pharmacol.* **1999**, *58*, 787−796.
(85) Mancy, A.; Broto, P.; Dijols, S.; Dansette, P. M.; Mansuy, D. The Substrate-Binding Site of Human Liver Cytochrome-P450 2C9 - An Approach using Designed Tienilic Acid-Derivatives and Molecular Modeling. *Biochemistry* **1995**, *34*, 10365−10375.
(86) Hutzler, J. M.; Balogh, L. M.; Zientek, M.; Kumar, V.; Tracy, T. S. Mechanism-Based Inactivation of Cytochrome P450 2C9 by Tienilic Acid and (±)-Suprofen: A Comparison of Kinetics and Probe Substrate Selection. *Drug Metab. Dispos.* **2009**, *37*, 59−65.